[3]. However, in the paper under discussion [2], the contribution of grain-boundary sliding to the total deformation should vary significantly over the stress levels, as reflected in the deformation rates, considered. The information on the ratio of the grain-boundary sliding component of deformation to the total deformation is presently being generated at this laboratory. The applied tensile stress used in Equations 1 and 2 is the stress normal to the cracked grain boundary, σ_n, rather than the tensile stress applied to a polycrystalline specimen, σ_a. In the case of steady-state creep for which Equations 1 and 2 are primarily concerned, one may reasonably assume that $\sigma_n \simeq \sigma_a$. The data of Nahm *et al* however, are for deformation rates which cover nearly six orders of magnitude, and include both tensile and creep results, so that this assumption is not necessarily justified for all deformation rates. This circumstance, then, requires that the angular orientation of the cracked grain boundaries with respect to the direction of the stress applied to the entire polycrystalline specimen either be known or assumed to confidently apply Equation 2 to all of the results. For crack angular orientations of less than about 80 to 90° to the applied stress direction, as observed in the tensile specimens, a significant shear stress component must be considered in addition to the normal stress component to explain the crack growth behaviour. It is also recognized that the cracks which develop during the deformation of polycrystalline materials at elevated temperatures are actually three-dimensional, rather than simply two-dimensional. It was for these reasons, in addition to the results obtained by Nahm *et al*, that the suggestion was made that the change in crack *volume*, i.e. in the amount of damage produced during the deformation process, and not just the change in crack *length*, as a function of time, may best represent the crack growth behaviour of the 304 stainless steel investigated.

In summary, we agree with Evans' [1] contention that the correct theoretical model must be applied only to the appropriate physical circumstances. We believe, however, that the analysis by Williams [3] is not appropriate to adequately describe all of the results given in the paper in question. Clearly, the analysis by Evans [5] is not appropriate for these results either. The data do indicate that a new approach, possibly based on features from either both or other types of models, be considered to explain all of the results by Nahm *et al* [2] consistent with the physical circumstances. This possibility is being explored by the authors.

Acknowledgement

This work was supported by the US Atomic Energy Commission under Contract AT(11-1)-2107.

References

1. H. E. EVANS, *J. Mater. Sci.* **8** (1973) 1827.
2. H. NAHM, D. J. MICHEL and J. MOTEFF, *ibid* **8** (1973) 104.
3. J. A. WILLIAMS, *Phil. Mag.* **15** (1967) 1289.
4. A. H. COTTRELL, *Trans. AIME* **212** (1958) 192.
5. H. E. EVANS, *Phil. Mag.* **23** (1971) 1101.

Received and accepted 13 July 1973.

H. NAHM
D. J. MICHEL*
J. MOTEFF
Department of Materials Science and Metallurgical Engineering, University of Cincinnati, Cincinnati, Ohio 45221 USA

*Present address: Naval Research Laboratory, Washington DC20375

Transverse compressive properties of an unbonded model cermet

In a previous paper [1], the transverse tensile properties of an unbonded model composite were found, in the belief that the behaviour of the model would indicate the type of variations in behaviour that might be expected in real materials. However, such materials might be used in compression: for instance, nuclear fuel cermets could be stacked vertically in a thermonuclear pile, and a possible use for soft metal/carbon fibre composites is bearing material. Therefore, a comparable piece of work has been done to investigate the properties of a similar model in compression.

Fig. 1 shows the dimensions and patterns of the specimens made from aluminium $2\frac{1}{4}$ wt % magnesium alloy plate 12.7 mm thick. Volume fraction was varied by increasing the hole size, and silver steel plugs were force-fitted into the holes. All specimens were annealed at 300°C.

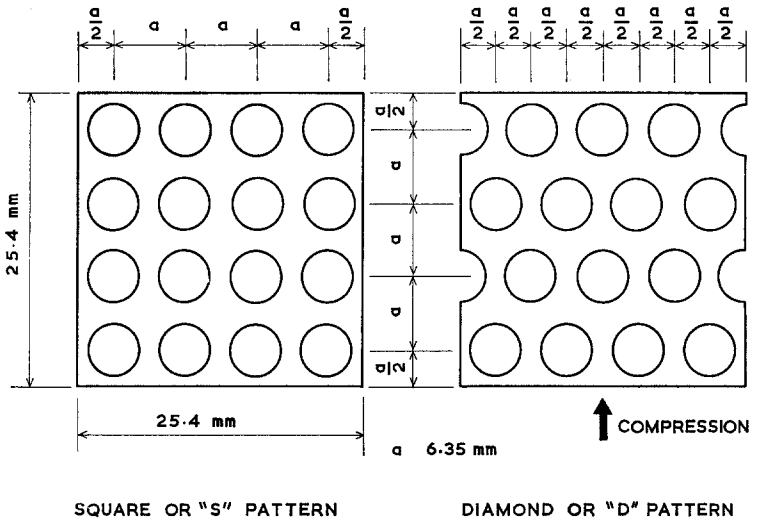

Figure 1 Size and shape of specimens.

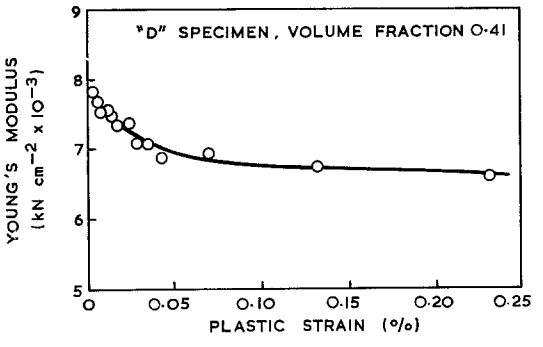

Figure 2 Modulus as a function of the amount of small plastic strain.

Two nominally identical specimens were tested for each result.

Young's modulus was measured by step loading and unloading, but was only accurate to $\pm 20\%$, although the results were reproducible on any one specimen to an accuracy of about 2%. As before, there was a small permanent set on the initial application of load, which increased with each increase in load, and the modulus decreased slightly with increasing permanent set (Fig. 2). The modulus at 0.2% plastic strain is given in Fig. 3. Other properties measured were the 0.2% proof stress, and the stress at 5% strain (Fig. 4). For comparison purposes, Figs. 3 and 4 show the corresponding tensile properties [1]. At high strains, the deformation was non-

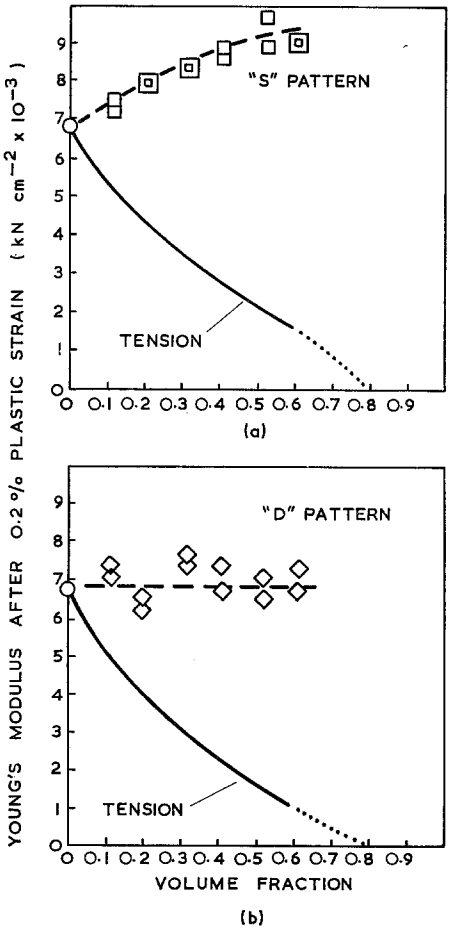

Figure 3 Modulus as a function of volume fraction.

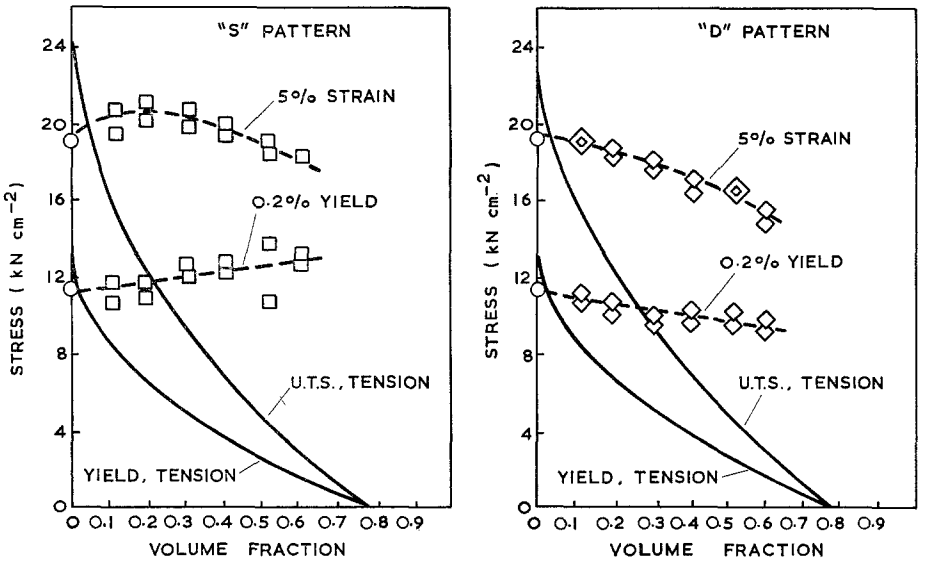

Figure 4 Strength as a function of volume fraction.

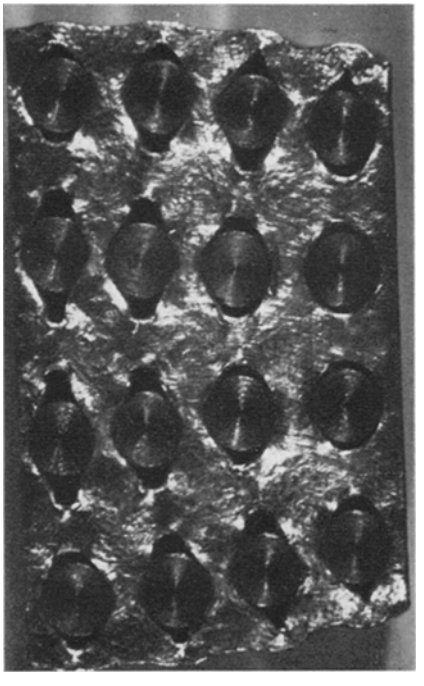

Figure 5 "S" pattern, volume fraction 0.3, compressed 21%.

uniform (Fig. 5), so it is possible that Figs. 3 and 4 are not truly representative of the properties of bulk materials of the same configurations. Within this context it is clear that:

1. Specimens with the "S" pattern are stronger than those with the "D" pattern (Fig. 4). This may be because the vertical webs in the "S" pattern (i.e. those whose plane of symmetry is vertical) are constrained to deform by multiple shear until buckling occurs, whereas in the webs of the "D" pattern whose planes of symmetry lie at an acute angle to the compression axis, one shear mode will be favoured.

2. In compression the cermets have a much higher modulus and strength than in tension.

3. The modulus and strength in compression are lower than those expected for a similar bonded cermet [2].

In tension, after a small amount of plastic strain, the specimens behaved as porous material of the same configuration [1]. In compression, the steel plugs bore a large part of the load. The steel plugs had a higher modulus and strength than the matrix, and were, in fact, not plastically deformed. Three other situations arise in which the modulus, the strength, or both properties of the included phase could be lower than those of the matrix. In all these cases, as long as the values of strength and modulus of the included phase are greater than zero, the included phase will always bear part of the load in compression, so that the modulus and strength of the unbonded composite will be greater here than in tension. However, as the "D" pattern is nearer to the configuration of the

real materials [1], these properties in compression will probably decline with increasing volume fraction.

References

1. B. R. BUTCHER, *J. Mater. Sci.* 7 (1972) 877.
2. I. L. MOGFORD, *Met. Rev.* **12** (1967) 49.

Received 15 June
and accepted 11 July 1973

B. R. BUTCHER
Metallurgy Division, AERE,
Harwell, Didcot, Berks, UK

A capacitance gauge for microstrain measurement in tension

In the period since 1960 several high sensitivity (i.e. $\leqslant 2 \times 10^{-6}$) strain measuring techniques have been utilized to study micro-yielding in materials. These include resistance [1-3], optical [4] and capacitance [5-7] gauges and linear variable differential transformers [8, 9]. Of these methods, the Tuckerman optical gauge allows a direct reading of strain, while the other techniques require a prior- and post-test calibration. All the techniques require precise temperature control or compensation and are applicable (when mounted on the specimen gauge length) within limited and different temperature ranges. In addition, operation of both optical and resistance gauges is difficult at strain-rates $\geqslant 10^{-3}$ sec^{-1}. Consequently, more than one strain measuring technique may be required, either to obtain microstrain data over a range of temperature and strain-rate or for calibration, and it is desirable to have available two systems which can be mounted interchangeably on the same test specimen. In this note we wish to report a new capacitance gauge design, which has the advantage that it is suitable for use, together with the Tuckerman optical gauge, on the gauge length of a tensile test specimen with a rectangular cross-section (Fig. 1).

The capacitance gauge, which is shown in Figs. 2a and b, consists essentially of a parallel plate capacitor, with an active plate containing a foil ring concentric with the specimen, and a ground plate, which is mounted directly onto the test specimen with spring loaded grips. The active foil is insulated on both sides with a thin layer of Araldite by two guard rings, while the ground plate is seated on a micrometer thread to allow a variation of the initial plate separation. The gauge is connected to a Wayne Kerr DM 100B distance meter by a double shielded cable, with the first and second shields attached to the guard rings and adjustable ground plate, respectively.

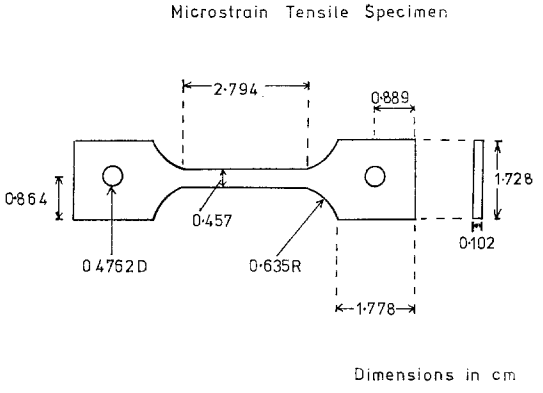

Figure 1 Test specimen for microstrain measurement in tension.

The absolute capacitance (C_g) of the gauge is given by:

$$C_g = \epsilon\pi \frac{Dt}{d} \quad (1)$$

where ϵ is the permittivity of air, D is the diameter of the active foil ring, t is the foil thickness and d is the plate separation. The design of the Wayne Kerr distance meter ensures that, provided $C_g \sim C_m$ (the capacitance of the meter) = 0.35 pF, then the output from the meter is inversely proportional to C_g and, hence, directly proportional to d. Another limit on the dimensions of the gauge is the requirement that $D > 1.67 \times 10^{-2}$ m (the specimen shoulder width). As the variation of C_g with d is given by:

$$\frac{\partial C_g}{\partial d} = -\epsilon\pi \frac{Dt}{d^2} \quad (2)$$

it is also desirable that the initial plate separation (d_0) should be small. The fixed gauge dimensions selected to best satisfy these conditions were $D = 2.25 \times 10^{-2}$ m and $t = 2.5 \times 10^{-5}$ m, which with an initial plate separation (d_0) of 5×10^{-5} m gave a gauge capacitance (C_g) of 0.31 pF.